

MONTE CARLO STUDY OF FOUR-SPINON DYNAMIC STRUCTURE FUNCTION IN ANTIFERROMAGNETIC HEISENBERG MODEL

A. Abada*

*Département de Physique, Ecole Normale Supérieure,
BP 92 Vieux-Kouba, Alger 16050, Algeria*

B. Si-Lakhal†

Département de Physique, Université de Blida, BP 270 Blida 09000, Algeria

(Dated: November 20, 2018)

Abstract

Using Monte Carlo integration methods, we describe the behavior of the exact four-spinon dynamic structure function S_4 in the antiferromagnetic spin 1/2 Heisenberg quantum spin chain as a function of the neutron energy ω and momentum transfer k . We also determine the four-spinon continuum, the extent of the region in the (k, ω) plane outside which S_4 is identically zero. In each case, the behavior of S_4 is shown to be consistent with the four-spinon continuum and compared to the one of the exact two-spinon dynamic structure function S_2 . Overall shape similarity is noted.

PACS numbers: 75.10.Jm 75.10.Pq 71.45.Gm 28.20.Cz 02.20.Uw

Keywords: Heisenberg spin chain. exact dynamic structure function.

*Electronic address: abada@wissal.dz

†Electronic address: silakhal@wissal.dz

I. INTRODUCTION

The spin $s = \frac{1}{2}$ Heisenberg quantum spin chain describes the magnetic properties of quasi-one-dimensional antiferromagnetic compounds like KCuF_3 [1]. The spin dynamics is experimentally investigated using inelastic neutron scattering [2]. From a theoretical standpoint, the quantity of interest is the dynamic structure function (DSF) S of two local spin operators. This is because the magnetic scattering cross section per magnetic site is directly proportional to it [3].

The Heisenberg model has been studied quite intensively [4, 5], and because of the presence of the $U_q(\widehat{\mathfrak{sl}}_2)$ symmetry [6], a number of exact results are available. Static properties need only the Yang-Baxter relation [5], whereas dynamic correlation functions require the additional notion of vertex operators and exploit bosonization methods [7]. One thus obtains compact expressions for form factors [6].

Regarding the dynamic structure function, the focus has so far been on S_2 , the two-spinon contribution to the total S . First there has been the Anderson (semi-classical) spin-wave theory [8], an approach based on an expansion in powers of $1/s$ and hence, exact only in the classical limit $s = \infty$. It can describe with some satisfaction compounds with higher spins [9], but fails in the quantum limit $s = \frac{1}{2}$. For this latter system, the Müller ansatz has been proposed, built mainly from finite-chain calculations and symmetry considerations [10]. It is an approximate expression for S_2 that accounts satisfactorily for many aspects of the phenomenology [2]. More recently, an exact expression for S_2 has been obtained, making extensive use of the $U_q(\widehat{\mathfrak{sl}}_2)$ symmetry [11], and a comparison with the Müller ansatz shows that it gives a better account of the data [12, 13].

Beyond the two-spinon DSF S_2 are of course all the other $S_{2p>2}$ contributions. The first one to look at is the four-spinon dynamic structure function S_4 , and the purpose of the present article is to describe its behavior. An exact expression for S_4 has been derived in [14], see also [15]. We intend to use that expression to describe the behavior of S_4 as a function of the neutron energy transfer ω and neutron momentum transfer k .

We must mention that a preliminary investigation into the behavior of S_4 has already been initiated in [16]. There we have used quadratures to perform the integrations involved in the expression of S_4 . But because of slow convergence of the algorithms we wrote, we could describe the behavior of S_4 only as a function of k , and only for relatively small values

of ω . In the present work, the integrations are performed using Monte Carlo methods, and this makes it possible not only to study S_4 as a function of k for a wider range of values of ω , but obtain a description of S_4 as a function of ω for a wide range of values of k as well. It is however important to note that, for the same values of ω , the behavior of S_4 as a function of k we obtain here by Monte Carlo methods is similar and consistent with the one we obtained in [16] using quadratures.

Also, we systematically carry a comparison of each result we obtain regarding S_4 to a corresponding one regarding S_2 . The reason is that there is good familiarity in the literature with the two-spinon DSF and so, such a comparison allows faster acquaintance with the four-spinon contribution. To have the discussion as clear as possible, we scale both S_4 and S_2 to one. All results concerning S_2 are already known [11, 12]; only those concerning S_4 are new.

This article is organized as follows. After these introductory remarks, we describe in the next section the Heisenberg model and give the definition of the dynamic structure function. We write its decomposition in $2p$ -spinon contributions and give the expressions of S_2 and S_4 . In section three, we first determine the four-spinon continuum, the region in the (k, ω) plane outside which S_4 is identically zero. We will see that it extends beyond the spin-wave des Cloizeaux and Pearson boundaries. To the best of our knowledge, this result is a first direct and explicit exact theoretical confirmation that the total S for the infinite chain tails outside the spin-wave continuum. Next in this section is a description of the behavior of S_4 as a function of ω for fixed values of k followed by a comparison with the corresponding behavior of S_2 . It is seen that there is consistency with the four-spinon continuum and that the overall shape (not the details) of S_4 is similar to the one of S_2 , each in its own respective continuum. Last is carried a description of the behavior of S_4 as a function of k for fixed values of ω and a comparison with the corresponding one of S_2 . Here too similarity between the two overall shapes is found as well as consistency with the four-spinon continuum. Section four includes concluding remarks and indicates few directions in which this work can be carried forward.

This paper is a continuation of the work [14]. We use the same notation except for a slight modification in (2.18) where here we introduce the function h instead of the function f with the relation $f \equiv \exp(-h)$.

II. FOUR-SPINON DYNAMIC STRUCTURE FUNCTION

The antiferromagnetic spin- $\frac{1}{2}$ XXX Heisenberg chain is defined as the isotropic limit of the XXZ anisotropic Heisenberg Hamiltonian:

$$H = -\frac{1}{2} \sum_{n=-\infty}^{\infty} (\sigma_n^x \sigma_{n+1}^x + \sigma_n^y \sigma_{n+1}^y + \Delta \sigma_n^z \sigma_{n+1}^z) . \quad (2.1)$$

$\Delta = (q + q^{-1})/2$ is the anisotropy parameter and the isotropic antiferromagnetic limit is obtained as $\Delta \rightarrow -1^-$, or equivalently $q \rightarrow -1^-$. Here $\sigma_n^{x,y,z}$ are the usual Pauli matrices acting at the site n of the chain. The exact diagonalization of this Hamiltonian is performed directly in the thermodynamic limit. This is necessary if we want to exploit the $U_q(\widehat{\mathfrak{sl}}_2)$ quantum group symmetry present in the model [6]. One consequence is the appearance of two vacuum states $|0\rangle_i$, $i = 0, 1$ due to two different boundary conditions on the infinite chain. The Hilbert space \mathcal{F} consists of n -spinon energy eigenstates $|\xi_1, \dots, \xi_n\rangle_{\epsilon_1, \dots, \epsilon_n; i}$ such that:

$$H|\xi_1, \dots, \xi_n\rangle_{\epsilon_1, \dots, \epsilon_n; i} = \sum_{j=1}^n e(\xi_j) |\xi_1, \dots, \xi_n\rangle_{\epsilon_1, \dots, \epsilon_n; i} , \quad (2.2)$$

where $e(\xi_j)$ is the energy of spinon j and ξ_j is a spectral parameter living on the unit circle. In the above relation, $\epsilon_j = \pm 1$. The translation operator T which shifts the spin chain by one site acts on the energy eigenstates in the following manner:

$$T|\xi_1, \dots, \xi_n\rangle_{\epsilon_1, \dots, \epsilon_n; i} = \prod_{i=1}^n \tau(\xi_i) |\xi_1, \dots, \xi_n\rangle_{\epsilon_1, \dots, \epsilon_n; 1-i} , \quad (2.3)$$

where $\tau(\xi_j) = e^{-ip(\xi_j)}$ and $p(\xi_j)$ is the lattice momentum of spinon j . The exact expressions of the spinon energy and lattice momentum in terms of the spectral parameter are known in the literature [6, 14, 17]. We are interested in their XXX limit and it is given below in eq (2.12). The completeness relation in \mathcal{F} reads:

$$\mathbf{I} = \sum_{i=0,1} \sum_{n \geq 0} \sum_{\{\epsilon_j = \pm 1\}_{j=1,n}} \frac{1}{n!} \oint \prod_{j=1}^n \frac{d\xi_j}{2\pi i \xi_j} |\xi_1, \dots, \xi_n\rangle_{\epsilon_1, \dots, \epsilon_n; i} \langle \xi_1, \dots, \xi_n | . \quad (2.4)$$

The two-point dynamic structure function is defined as the Fourier transform of the zero-temperature vacuum-to-vacuum two-point function. The transverse DSF is therefore defined by:

$$S^{i,+}(\omega, k) = \int_{-\infty}^{\infty} dt \sum_{m \in \mathbb{Z}} e^{i(\omega t + km)} \langle 0 | \sigma_m^+(t) \sigma_0^-(0) | 0 \rangle_i , \quad (2.5)$$

where ω and k are the neutron energy and momentum transfer respectively, and σ^\pm denotes $(\sigma^x \pm i\sigma^y)/2$. The DSF satisfies the following relations:

$$S^{i,+}(\omega, k) = S^{i,+}(\omega, -k) = S^{i,+}(\omega, k + 2\pi), \quad (2.6)$$

expressing reflection symmetry and periodicity. Inserting the completeness relation (2.4) and using the Heisenberg relation:

$$\sigma_m^{x,y,z}(t) = \exp(iHt) T^{-m} \sigma_0^{x,y,z}(0) T^m \exp(-iHt), \quad (2.7)$$

we can write the transverse DSF as the sum of n -spinon contributions:

$$S^{i,+}(\omega, k) = \sum_{n \text{ even}} S_n^{i,+}(\omega, k), \quad (2.8)$$

where the n -spinon DSF S_n is given by:

$$\begin{aligned} S_n^{i,+}(\omega, k) &= \frac{2\pi}{n!} \sum_{m \in \mathbb{Z}} \sum_{\epsilon_1, \dots, \epsilon_n} \oint \prod_{j=1}^n \frac{d\xi_j}{2\pi i \xi_j} e^{im(k + \sum_{j=1}^n p_j)} \delta\left(\omega - \sum_{j=1}^n e_j\right) \\ &\times X_{\epsilon_n, \dots, \epsilon_1}^{i+m}(\xi_n, \dots, \xi_1) X_{\epsilon_1, \dots, \epsilon_n}^{1-i}(-q\xi_1, \dots, -q\xi_n), \end{aligned} \quad (2.9)$$

a relation in which X^i denotes the form factor:

$$X_{\epsilon_1, \dots, \epsilon_n}^i(\xi_1, \dots, \xi_n) \equiv {}_i\langle 0 | \sigma_0^+ (0) | \xi_1, \dots, \xi_n \rangle_{\epsilon_1, \dots, \epsilon_n; i}. \quad (2.10)$$

In relation (2.9), $i + m$ is to be read modulo 2. Note that each S_n satisfies the symmetry relations (2.6).

An exact expression for the form factor X^i is known [6, 18]. To arrive at the result, one has to exploit extensively the infinite-dimensional representation of $U_q(\widehat{\mathfrak{sl}}_2)$ and bosonize the relevant vertex operators in order to be able to manipulate in a systematic way traces of these operators which ultimately yield the correlation functions. Using this form factor, it is possible to give an exact expression for the n -spinon DSF in the anisotropic case [14] and determine its isotropic limit [15], obtained via the replacement [6, 14]:

$$\xi = ie^{-2i\epsilon\rho}; \quad q = -e^{-\epsilon}, \quad \epsilon \rightarrow 0^+, \quad (2.11)$$

where ρ becomes the spectral parameter suited for this limit. The expressions of the energy e and momentum p in terms of ρ then read:

$$e(\rho) = \frac{\pi}{\cosh(2\pi\rho)} = -\pi \sin p; \quad \cot p = \sinh(2\pi\rho); \quad -\pi \leq p \leq 0. \quad (2.12)$$

It turns out that the transverse two-spinon DSF S_2 does not involve a contour integration, see (2.9). Its exact expression has been derived in [11]. It reads:

$$S_2^{+-}(\omega, k - \pi) = \frac{1}{4} \frac{e^{-I(\rho)}}{\sqrt{\omega_{2u}^2 - \omega^2}} \Theta(\omega - \omega_{2l}) \Theta(\omega_{2u} - \omega), \quad (2.13)$$

where Θ is the Heaviside step function and the function $I(\rho)$ is given by:

$$I(\rho) = \int_0^{+\infty} \frac{dt \cosh(2t) \cos(4\rho t) - 1}{t \sinh(2t) \cosh(t)} e^t. \quad (2.14)$$

$\omega_{2u(l)}$ is the upper (lower) bound of the two-spinon excitation energies called the des Cloizeaux and Pearson (dCP) [10, 11] upper (lower) bound or limit. They read:

$$\omega_{2u} = 2\pi \sin \frac{k}{2}; \quad \omega_{2l} = \pi |\sin k|. \quad (2.15)$$

The quantity ρ is related to ω and k by the relation:

$$\cosh \pi \rho = \sqrt{\frac{\omega_{2u}^2 - \omega_{2l}^2}{\omega^2 - \omega_{2l}^2}}, \quad (2.16)$$

which is obtained using eq (2.12) and the energy-momentum conservation laws. The properties of S_2 have been discussed in [12, 13] where a comparison with the Müller ansatz [10] is carried.

The four-spinon DSF S_4 involves only one contour integration and its expression is given in [14]. For $0 \leq k \leq \pi$ it reads:

$$S_4^{+-}(\omega, k - \pi) = C_4 \int_{-\pi}^0 dp_3 \int_{-\pi}^0 dp_4 F(\rho_1, \dots, \rho_4). \quad (2.17)$$

For other values of k , it extends by symmetry using (2.6). C_4 is a numerical constant irrelevant for the present work since we will scale S_4 to unity, and the integrand F is given by:

$$F(\rho_1, \dots, \rho_4) = \sum_{(p_1, p_2)} \frac{\exp[-h(\rho_1, \dots, \rho_4)] \sum_{\ell=1}^4 |g_\ell(\rho_1, \dots, \rho_4)|^2}{\sqrt{W_u^2 - W^2}}. \quad (2.18)$$

The different quantities involved in this expression are as follows.

$$\begin{aligned} W &= \omega + \pi (\sin p_3 + \sin p_4); \\ W_u &= 2\pi |\sin (K/2)|, \quad K = k + p_3 + p_4; \\ \cot p_j &= \sinh(2\pi \rho_j), \quad -\pi \leq p_j \leq 0. \end{aligned} \quad (2.19)$$

The function h is given by:

$$h(\rho_1, \dots, \rho_4) = \sum_{1 \leq j < j' \leq 4} I(\rho_{jj'}), \quad (2.20)$$

where $\rho_{jj'} = \rho_j - \rho_{j'}$ and the function g_ℓ reads:

$$g_\ell = (-1)^{\ell+1} (2\pi)^4 \sum_{j=1}^4 \cosh(2\pi\rho_j) \times \sum_{m=\Theta(j-\ell)}^{\infty} \frac{\prod_{i \neq \ell} (m - \frac{1}{2}\Theta(\ell - i) + i\rho_{ji})}{\prod_{i \neq j} \pi^{-1} \sinh(\pi\rho_{ji})} \prod_{i=1}^4 \frac{\Gamma(m - \frac{1}{2} + i\rho_{ji})}{\Gamma(m + 1 + i\rho_{ji})}, \quad (2.21)$$

where Θ is the Heaviside step function. In (2.18), the sum $\sum_{(p_1, p_2)}$ is over the two pairs (p_1, p_2) and (p_2, p_1) solutions of the energy-momentum conservation laws:

$$W = -\pi(\sin p_1 + \sin p_2); \quad K = -p_1 - p_2. \quad (2.22)$$

They read:

$$(p_1, p_2) = (-K/2 + \arccos(W/[2\pi \sin(K/2)]), -K/2 - \arccos(W/[2\pi \sin(K/2)]). \quad (2.23)$$

Note that the solution in (2.23) is allowed as long as $W_l \leq W \leq W_u$ where W_u is given in (2.19) and:

$$W_l = \pi |\sin K|. \quad (2.24)$$

The (analytic) behavior of the function F in (2.18) is discussed in [14]. It is shown that the series g_ℓ is convergent. It is also shown that g_ℓ stays finite when two ρ_i 's or more get equal. Since the function $\exp(-h)$ goes to zero in these regions [12], the integrand F of S_4 is regular there. Furthermore, it is shown that F is exponentially convergent when one of the ρ_i 's goes to infinity, which means the two integrals over p_3 and p_4 in (2.17) do not yield infinities. All these analytic results help secure safe numerical manipulations.

III. BEHAVIOR OF EXACT FOUR-SPINON DSF

From now on, we restrict ourselves to the interval $0 \leq k \leq \pi$. All forthcoming results can be carried to the other intervals of k using the symmetry relations (2.6). Also, we scale both S_4 and S_2 to appropriate units in order to display conveniently their respective behaviors.

A. Four-spinon continuum

The first feature we discuss is the ‘four-spinon continuum’, by analogy with the two-spinon (or the spin-wave) continuum. It is the extent of the region in the (k, ω) -plane outside which S_4 is identically zero. Remember that from (2.13), S_2 is confined to the region $\omega_{2l}(k) \leq \omega \leq \omega_{2u}(k)$, where $\omega_{2l,u}(k)$ are the dCP boundaries given in (2.15). From the condition $W_l \leq W \leq W_u$ mentioned after (2.23), we deduce that in order for S_4 to be nonzero identically, we must have $\omega_{4l}(k) \leq \omega \leq \omega_{4u}(k)$, where:

$$\begin{aligned}\omega_{4l}(k) &= 3\pi \sin(k/3) \quad \text{for } 0 \leq k \leq \pi/2; \\ \omega_{4l}(k) &= 3\pi \sin(k/3 + 2\pi/3) \quad \text{for } \pi/2 \leq k \leq \pi; \\ \omega_{4u}(k) &= 4\pi \cos(k/4) \quad \text{for } 0 \leq k \leq \pi.\end{aligned}\tag{3.1}$$

We see that $\omega_{4l}(k)$ and $\omega_{4u}(k)$ are a sort of four-spinon dCP boundaries for S_4 . The two and four-spinon continua are drawn in figure 1 below. We immediately notice that the four-spinon continuum is not restricted to the region between the two-spinon dCP branches, which means, a fortiori, that the full S is also not confined to the spin-wave continuum. This is a direct and explicit theoretical confirmation of the ‘tail’ of the dynamic structure function observed outside the spin-wave continuum in finite-chain numerical calculations [10] and the phenomenology [2]. Due to the six and higher spinon contributions, it is actually legitimate to expect the full DSF to tail even further outside the four-spinon continuum, with arguably much smaller values. For example, in the interval $0 \leq k/\pi < 0.51741$, there is a narrow region between ω_{2u} and ω_{4l} inside which both S_2 and S_4 are identically zero whereas the total S may have (very small) nonzero values, something that could eventually be checked in finite-chain calculations. However, it is not possible to estimate exactly the continua corresponding to the $S_{n>4}$ without manageable explicit formulae for these. But what is already clear from our study is the fact that indeed, the spin-wave continuum is not restrictive to the total dynamic structure function.

There are further general features we can also read from figure 1 without having recourse to detailed calculations. For example, we see that inside the interval $0 \leq k/\pi < 0.51741$, the four-spinon continuum lies entirely above the two-spinon continuum. This means that for this interval, S_2 may be accepted as a good approximation for the total S between the spin-wave boundaries and S_4 between ω_{4l} and ω_{4u} . For $0.51741 \leq k/\pi \leq 1$ however and as k



FIG. 1: Four-spinon (full) and two-spinon (dashed) continua.

increases, there is increasing overlap between the two continua so that inside the spin-wave continuum, we may expect S to divert in perhaps a non-negligible way from S_2 .

B. Behavior as a function of the energy transfer

Next we describe the behavior of S_4 as a function of ω for fixed values of k . Figure 2 displays the shapes of S_4 for respectively $k/\pi = 1/4, 1/2, 3/4$ and 1. As an illustration, take for example the case $k/\pi = 1/4$. We see on figure 2 that S_4 is zero until $\omega/\pi \simeq 0.68$, which corresponds to the beginning of the four-spinon continuum $\omega_{4l}(\pi/4)/\pi = 3 \sin(\pi/12) = 0.77646$. We obtain a slightly smaller value when reading directly from figure 2 because of fitting. Note that it is important to check each time consistency with the four-spinon continuum. This is because the lower and upper branches $\omega_{4l,u}(k)$ are not imposed explicitly in the integration algorithm of S_4 unlike the case of S_2 where the corresponding expression (2.13) incorporates explicitly the two-spinon dCP boundaries $\omega_{2l,u}(k)$. For S_4 , only the conditions $W_l \leq W \leq W_u$ noted just before (2.24) are imposed.

Starting from $\omega/4\pi \simeq 0.17$, S_4 jumps sharply from zero to a maximum at $\omega/4\pi \simeq 0.21$ (read from figure 2). Then it decreases with two apparent local minima until it becomes

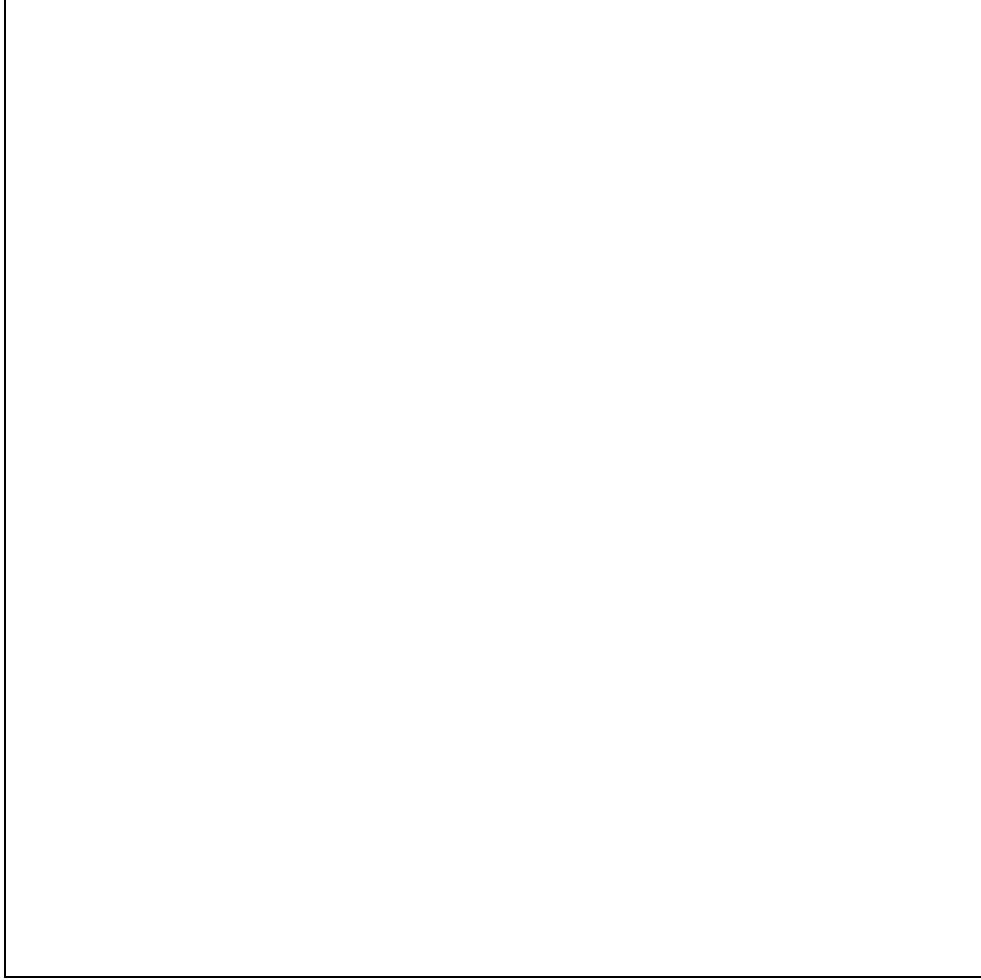


FIG. 2: (Scaled) S_4 as a function of ω for fixed k .

negligible at roughly $\omega/4\pi \simeq 0.6$. The upper branch of the four-spinon continuum at $k = \pi/4$ is $\omega_{4u}(\pi/4)/4\pi = \cos(\pi/16) = 0.9808$. Hence, S_4 is practically negligible (but not identically zero) for values of $\omega/4\pi$ between about 0.6 and 0.9808. The description of S_4 as a function of ω for the other values of k can be carried along the same lines and each time, consistency with the four-spinon continuum is checked. The shapes are all similar to one another: steep increase from zero to a maximum value, followed by a ‘wiggled’ slower decrease to zero.

Furthermore, it is interesting to notice that for all values of k , the overall shape of S_4 , *not* the detail, is roughly similar to the one of S_2 , represented as a function of ω for the same values of k in figure 3. For instance, for $k/\pi = 1/4$, S_2 starts very sharply at about $\omega/2\pi \simeq 0.35$, which corresponds to the start of the two-spinon continuum at $\omega_{2l}(\pi/4)/2\pi = 0.35355$. It reaches a maximum before decreasing more slowly towards zero.

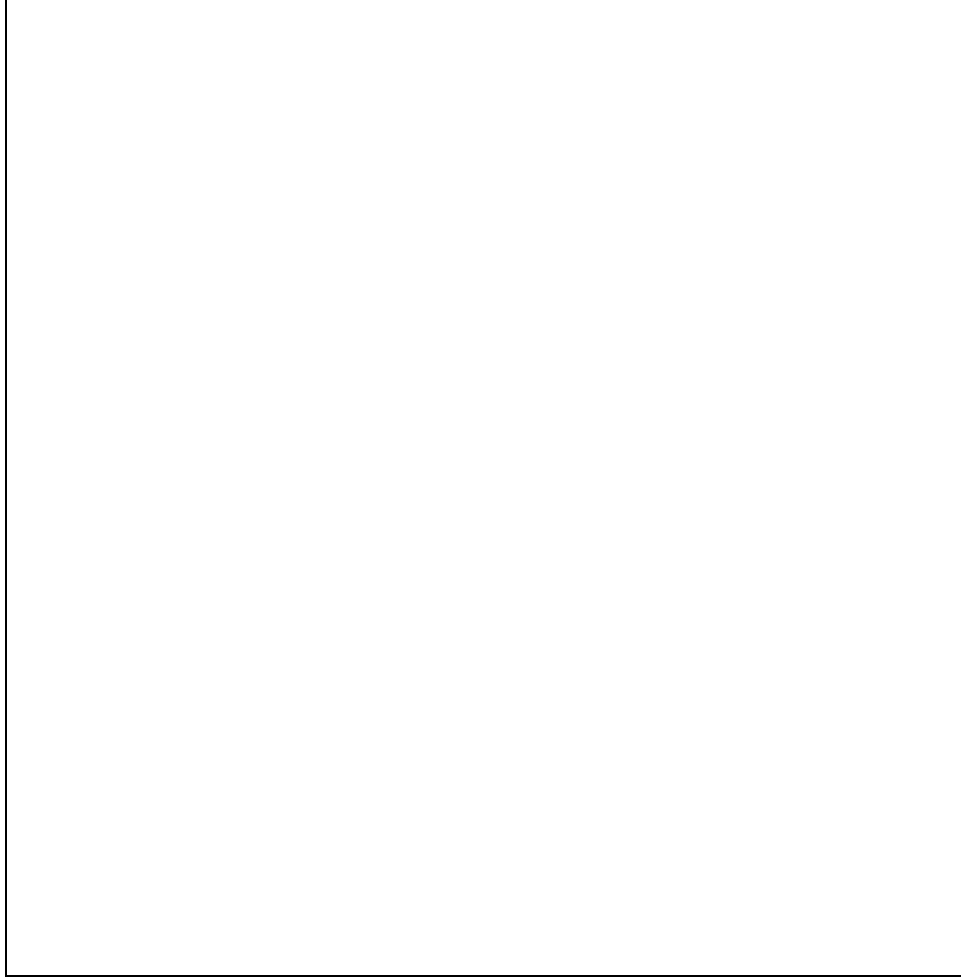


FIG. 3: (Scaled) S_2 as a function of ω for fixed k .

The only difference worth mentioning is the decrease of S_4 after its absolute maximum which presents local minima and maxima whereas the decrease of S_2 is always ‘smooth’. This may originate from the ‘richer’ structure of the expression of S_4 with respect to that of S_2 .

C. Behavior as a function of the momentum transfer

Last we describe the behavior of S_4 as a function of k for fixed values of ω . In figure 4 are plotted the graphs of S_4 in terms of k for $\omega/\pi = 1/4, 1/2, 3/4, 1$ respectively. Let us describe for example the case $\omega/\pi = 1/4$. We see on figure 4 that S_4 is zero until we reach the value $k/\pi \simeq 0.88$. On the other hand, the four-spinon continuum lies outside the interval $0.07967 \leq k/\pi \leq 0.92033$. In the region $0 \leq k/\pi \leq 0.07967$, figure 4 shows no

discernible finite values for S_4 , only a very thin ‘trace’ that would be more visible with a better resolution. This means that S_4 is negligible for those small values of k . For larger values of ω though, S_4 picks up clear finite values in the interval $0 \leq k \leq 3 \arcsin(\omega/3\pi)$; see the other graphs on figure 4. Those values get larger as ω increases.

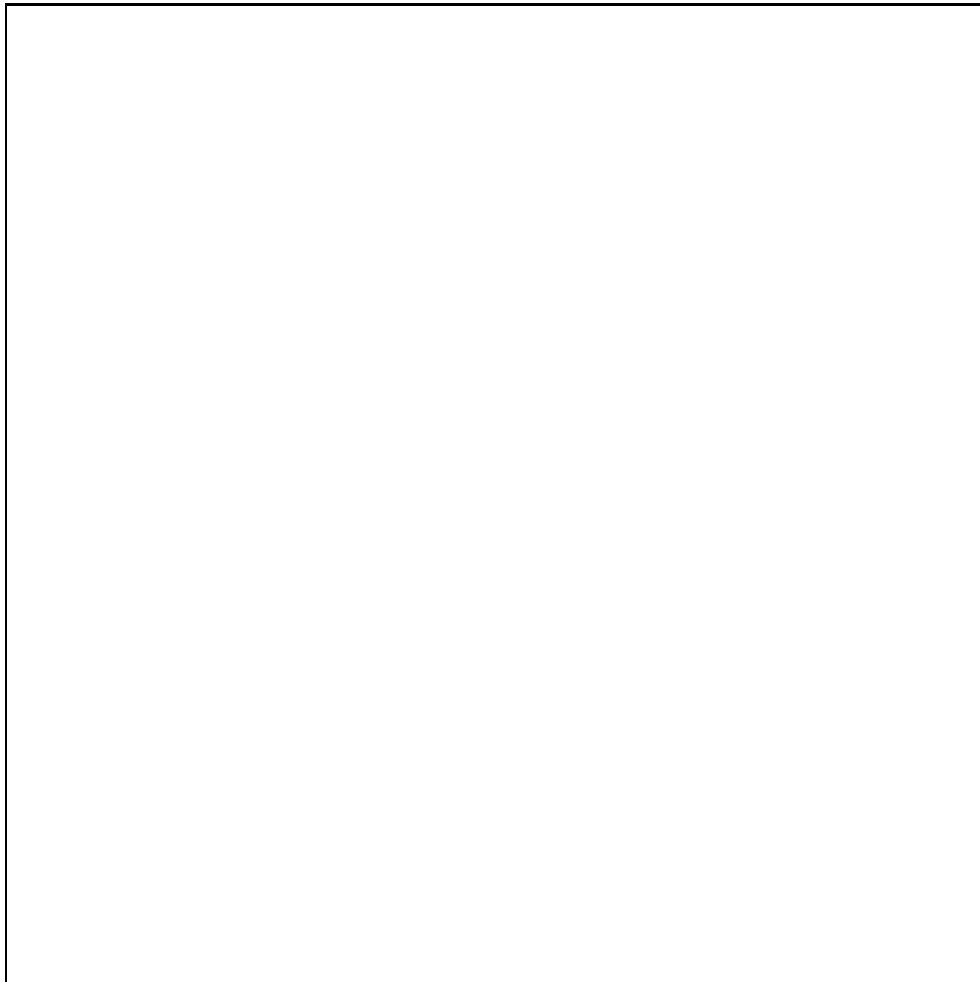


FIG. 4: (Scaled) S_4 as a function of k for fixed ω .

Returning to the case $\omega/\pi = 1/4$, we see that S_4 starts from zero at $k/\pi \simeq 0.88$ (slightly smaller than the exact value 0.92033 because of fitting), rises sharply to a maximum and then decreases. The behavior of S_4 for the other values of ω is also consistent with the four-spinon continuum. Take for example the case $\omega/\pi = 1/2$. The four-spinon continuum indicates that S_4 is identically zero for $0.1599 \leq k/\pi \leq 0.84008$. We see indeed small values for S_4 from $k/\pi = 0$ up to a little before 0.2, and S_4 rising again from zero a little after $k/\pi = 0.8$ to a local maximum, then to an absolute maximum before decreasing.

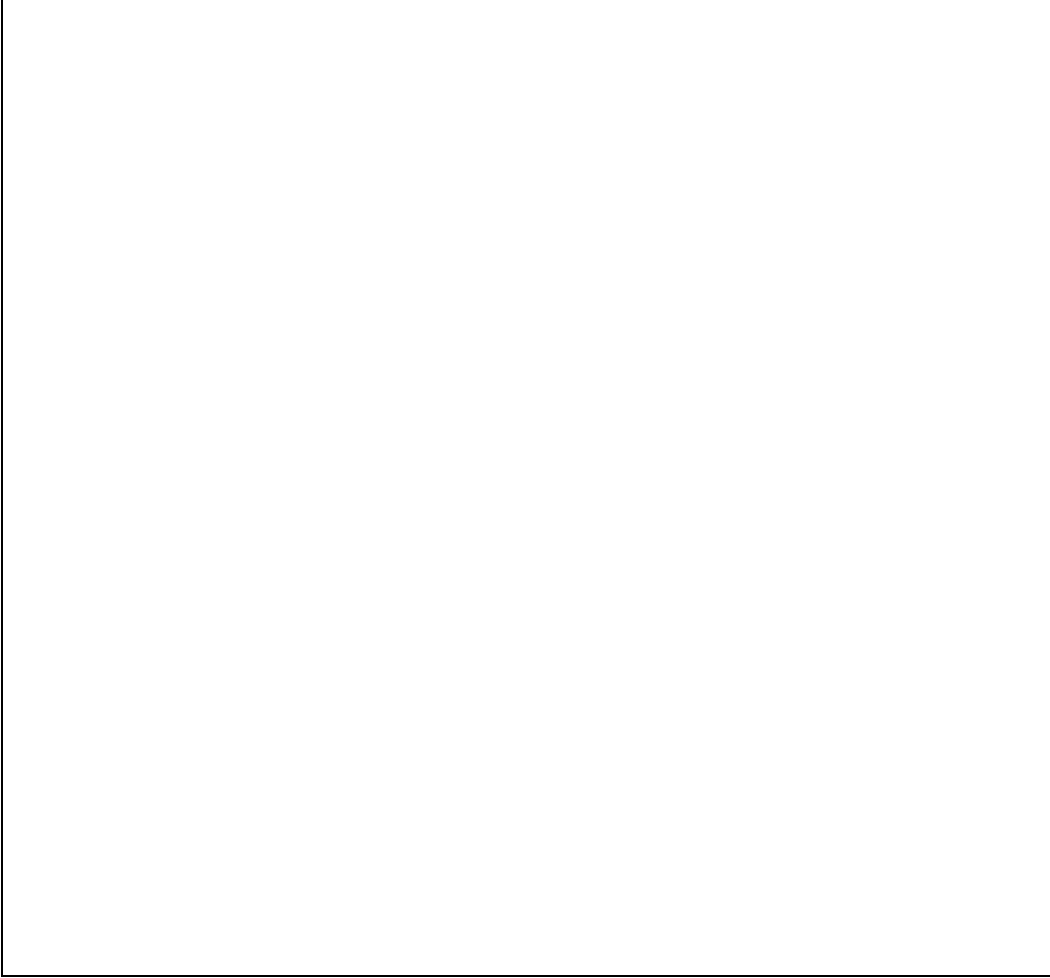


FIG. 5: (Scaled) S_2 as a function of k for fixed ω .

Here too S_2 has a similar overall behavior within its own (two-spinon) continuum. Figure 5 displays the behavior of S_2 with respect to k for the same fixed values of ω . But as ω increases, we notice the richer structure of S_4 with respect to the corresponding one for S_2 . This is due to the more involved expression of S_4 . In fact, for larger values of ω , the integrand F in (2.17) is nonvanishing in larger and larger areas in the (p_3, p_4) plane. For illustration, compare the behavior of F shown in figure 6 for $(k, \omega) = (0.5\pi, 2\pi)$ with the one shown in figure 7 for $(k, \omega) = (0.5\pi, 3\pi)$. In this regard, we recall that the quadrature-based algorithms written in [16] were based on this observation and took advantage of the fact that for fairly small values of ω , the integrand F was negligible in large areas of the (p_3, p_4) plane. This is the reason why those algorithms could not be carried to larger values of ω , or be able to describe efficiently a behavior as a function of the neutron energy ω itself. As



FIG. 6: The integrand F in (2.17) as a function of (p_3, p_4) for $(k, \omega) = (0.52\pi, 2\pi)$.

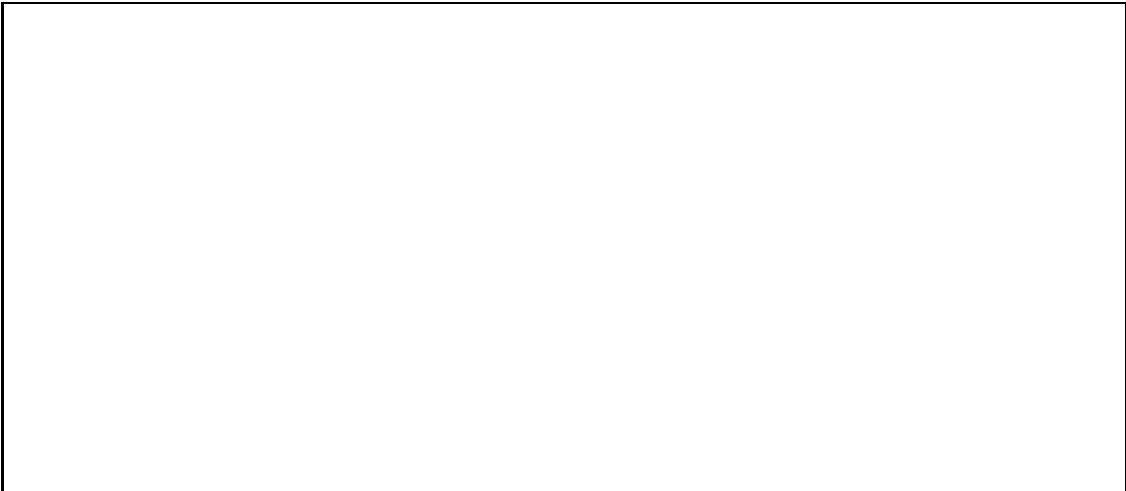


FIG. 7: The integrand F in (2.17) as a function of (p_3, p_4) for $(k, \omega) = (0.5\pi, 3\pi)$.

already mentioned, we have used here Monte Carlo techniques and we can do better, but consistency with [16] is realized, i.e., we have the same behavior of S_4 as a function of k for the same small values of ω .

IV. CONCLUSION

In this work, we have described the behavior of the exact four-spinon dynamic structure function S_4 in the antiferromagnetic isotropic Heisenberg quantum spin chain at zero tem-

perature as a function of the neutron energy ω and momentum transfer k . We have also determined the four spinon continuum, the region outside which S_4 is identically zero. The discussion was carried in the form of a comparison with the corresponding behavior of the exact two-spinon dynamic structure function S_2 , already known in the literature. Figures 8 and 9 summarize these two behaviors where S_4 (8) and S_2 (9) are drawn in the (k, ω) plane. Recall that we have scaled them down to one.

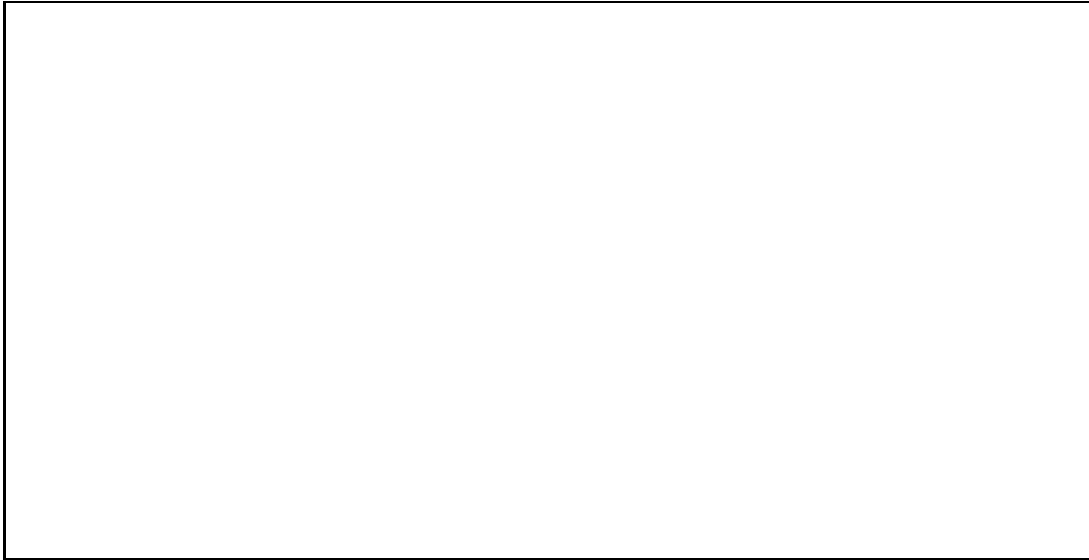


FIG. 8: (Scaled) S_4 as a function of k and ω .



FIG. 9: (Scaled) S_2 as a function of k and ω .

There are four directions in which one may wish to carry forward with this work. The first is the anisotropic case. The model is exactly soluble and we do have generic expressions for S_n in the form of contour integrals in the spectral parameters complex planes [15]. The difficulty here is that the integrands involve much more complicated functions which are already present in S_2 , and one should expect intricate complexities in this more general case.

The second direction in which one may want to push forward is the situation where there is an external magnetic field. There are finite-chain calculations in this regard, [10] and more recently the works [19]. But one has to remember that the model is not exactly solvable in this case. So one may want to try small perturbations around the zero-field limit solution. The third direction is the finite-temperature case. Here too there are finite-chain results and it is interesting to see those effects on S_2 and S_4 . The fourth direction is to look into the situation of a spin-one chain. The model is still exactly solvable and exploiting the quantum group symmetry, compact expressions for the form factors are available [20, 21, 22].

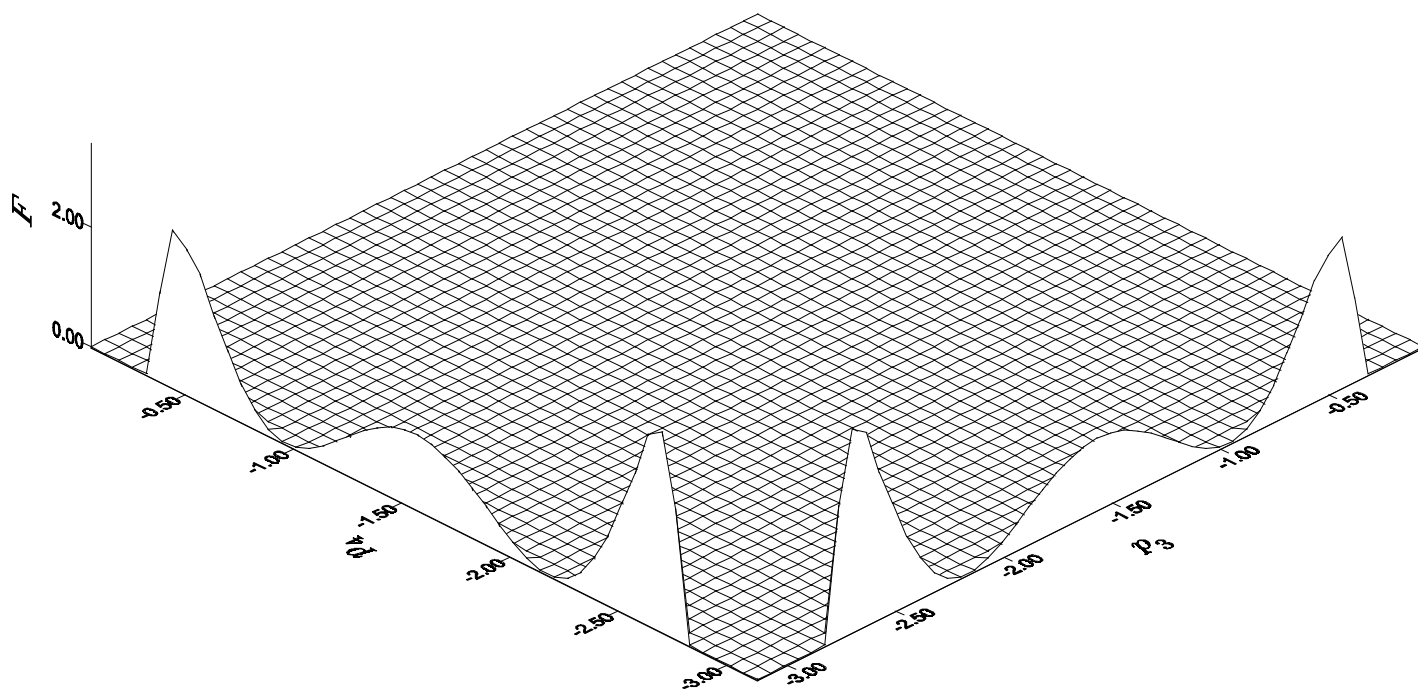
-
- [1] K. Hirakawa and Y. Kurogi, Prog. Theor. Phys. **S46** (1970) 147.
 - [2] D.A. Tennant, R.A. Cowley, S.E. Nagler and A.M. Tsvelik, Phys. Rev. **B52** (1995) 13368; D.A. Tennant, S.E. Nagler, D. Wetz, G. Shirane and K. Yamada, Phys. Rev. **B52** (1995) 13381; D.A. Tennant, T.G. Perring, R.A. Cowley and S.E. Nagler, Phys. Rev. Lett. **70** (1993) 4003; S.E. Nagler, D.A. Tennant, R.A. Cowley, T.G. Perring and S.K. Satija, Phys. Rev. **B44** (1991) 12361.
 - [3] G.L. Squires, ‘*Introduction to the theory of thermal neutron scattering*’, Cambridge University Press, 1996; S.W. Lovesey, ‘*Theory of neutron scattering from condensed matter*’, Clarendon, Oxford, 1987.
 - [4] Some (not *all*) of the literature related to the Heisenberg model comprises W. Heisenberg, Z. Phys. **49** (1928) 619; H. Bethe, Z. Phys. **71** (1931) 205; L. Hulthén, Arkiv. Mat. Astron. Fysik **A 1126** (1938) 1; E.H. Lieb and D.C. Mattis, J. Math. Phys. **3** (1962) 749; J. des Cloizeaux and J.J. Pearson, Phys. Rev. **128** (1962) 2131; R.B. Griffiths, Phys. Rev. **133** (1964) A 768; C.N. Yang and C.P. Yang, Phys. Rev. **150** (1966) 321; **150** (1966) 327; **151** (1966) 258; Th. Niemeijer, Physica **36** (1967) 377; E. Barouch, B.M. McCoy and D.B. Abraham, Phys. Rev.

- A4 (1971) 2331; M. Gaudin, Phys. Rev. Lett. 26 (1971) 1301; M. Takahashi, Prog. Theor. Phys. 46 (1971) 401; L.A. Takhtajan and L.D. Faddeev, Russ. Math. Surveys 34 (1979) 11; B.M. McCoy, J.H.H. Perk and R.E. Shrock, Nucl. Phys. B220 (1983) 35; O. Babelon, H.J. de Vega and C.M. Viallet, Nucl. Phys. B220 (1983) 13; G. Müller and R.E. Shrock, Phys. Rev. B29 (1984) 288; J.M.R. Roldan, B.M. McCoy and J.H.H. Perk, Physica 136A (1986) 255; V.E. Korepin, A.G. Izergin and N.M. Bogoliubov, ‘*The Quantum Inverse Scattering Method and Correlation Functions*’, Cambridge University Press, 1993; F.H.L. Essler, H. Frahm, A.G. Izergin and V.E. Korepin, Comm. Math. Phys. 174 (1994) 191; V.E. Korepin, A.G. Izergin, F.H.L. Essler and D. Uglov, Phys. Lett. A190 (1994) 182.
- [5] R.J. Baxter, ‘*Exactly Solved Models in Statistical Mechanics*’, Academic Press, 1982.
- [6] M. Jimbo and T. Miwa, ‘*Algebraic Analysis of Solvable Lattice Models*’, American Mathematical Society, 1994.
- [7] O. Davies, O. Foda, M. Jimbo, T. Miwa and A. Nakayashiki, Comm. Math. Phys. 151 (1993) 89; I.B. Frenkel and N.H. Jing, Proc. Natl. Acad. Sci. 85 (1988) 9373; A. Abada, A.H. Bougourzi and M.A. El Gradechi, Mod. Phys. Lett. A8 (1993) 715; A.H. Bougourzi, Nucl. Phys. B404 (1993) 457; A.H. Bougourzi, ‘*Bosonization of quantum affine groups and its application to the higher spin Heisenberg model*’, [q-alg/9706015](#).
- [8] P.W. Anderson, Phys. Rev. 86 (1952) 694.
- [9] M.T. Hutchings, G. Shirane, R.J. Birgeneau and S.L. Holt, Phys. Rev. B5, (1972) 1999.
- [10] G. Müller, H. Thomas, H. Beck and J.C. Bonner, Phys. Rev. B24 (1981) 1429.
- [11] A.H. Bougourzi, M. Couture and M. Kacir, Phys. Rev. B54 (1996) 12669.
- [12] M. Karbach, G. Müller and A.H. Bougourzi, ‘*Two-spinon dynamic structure factor of the one-dimensional $S = 1/2$ Heisenberg antiferromagnet*’, [cond-mat/9606068](#).
- [13] A.H. Bougourzi, M. Karbach and G. Müller, ‘*Exact two-spinon dynamic structure factor of the one-dimensional $s = 1/2$ Heisenberg-Ising antiferromagnet*’, [cond-mat/9712101](#).
- [14] A. Abada, A.H. Bougourzi and B. Si-lakhal, Nucl. Phys. B497 [FS] (1997) 733.
- [15] A.H. Bougourzi, Mod. Phys. Lett B10 (1996) 1237.
- [16] A. Abada, A.H. Bougourzi, B. Si-Lakhal and S. Seba, ‘*Four-Spinon Dynamical Correlation Function in Isotropic Heisenberg Model*’, [cond-mat/9802271](#), unpublished.
- [17] L.D. Faddeev and L.A. Takhtajan, J. Soviet. Math. 24 (1984) 241.
- [18] F.A. Smirnov, ‘*Form Factors in Completely Integrable Models of Quantum Field Theory*’

World Scientific, Singapore, 1992.

- [19] M. Karbach, D. Biegel and G. Müller, ‘*Quasiparticles governing the zero-temperature dynamics of the 1D spin-1/2 Heisenberg antiferromagnet in a magnetic field*’, `cond-mat/0205142`; M. Karbach and G. Müller, ‘*Line shape predictions via Bethe ansatz for the one dimensional spin-1/2 Heisenberg antiferromagnet in a magnetic field*’, `cond-mat/0005174`.
- [20] M. Idzumi, Int. J. Mod. Phys. **A9** (1994) 4449; ‘*Correlation functions of the spin 1 analog of the XXZ model*’, `hep-th/9307129`.
- [21] A.H. Bougourzi and R.A. Weston, Nucl. Phys. **B417** (1994) 439.
- [22] A.H. Bougourzi, ‘*Bosonization of quantum affine groups and its application to higher spin Heisenberg model*’, `q-alg/9706015`.

$k=0.5\pi$
 $\omega=2\pi$



$k=0.5\pi$
 $\omega=3\pi$

